

# Improving the Surface Integrity of Additive-Manufactured Metal Parts by Ultrasonic Vibration-Assisted Burnishing

Akinori Teramachi

Department of Mechanical Engineering,  
Faculty of Science and Technology,  
Keio University,  
Hiyoshi 3-14-1,  
Kohoku-ku, Yokohama 223-8522, Japan

Jiwang Yan<sup>1</sup>

Department of Mechanical Engineering,  
Faculty of Science and Technology,  
Keio University,  
Hiyoshi 3-14-1,  
Kohoku-ku, Yokohama 223-8522, Japan  
e-mail: yan@mech.keio.ac.jp

*Metal additive manufacturing (AM) has been attracting attention as a new manufacturing method, but a surface finishing process is usually needed to improve the surface quality. As a new surface finishing process, ultrasonic vibration-assisted burnishing (UVAB) is promising. In this study, UVAB was performed on an additive-manufactured AlSi10Mg workpiece to improve its surface/subsurface integrity. The effects of ultrasonic vibration (UV) and lateral tool pass width on the burnishing performance were investigated. It was observed that the surface roughness, filling ratio, and hardness of the surface layer were simultaneously improved after burnishing. This study shows the effectiveness of applying UVAB to improve the surface quality of additive-manufactured products for various industrial uses.* [DOI: 10.1115/1.4043344]

*Keywords:* ball burnishing, ultrasonic vibration, material void, additive manufacturing, surface finish, hardness

## 1 Introduction

In recent years, metal additive manufacturing (AM) has been attracting attention as a new manufacturing method because it can create products with highly complicated shapes and internal structures, as compared with products by conventional methods [1]. For example, three-dimensional internal structures in metallic molds can be fabricated by AM, which is useful to promote cooling effects [2]. However, AM metals have some drawbacks such as high surface roughness and internal defects, such as voids [3]. These problems result in a reduction in surface function and fatigue strength [4]. Although improving the AM performance is a solution, the quality of AM products is limited in principle [5]. Therefore, to use the AM products in high-requirement applications, subsequent finishing processes such as milling, polishing, blasting and heat treating are necessary [3]. However, a single method cannot solve the problems of surface roughness and internal voids simultaneously; thus, an alternative method is to be explored [6].

<sup>1</sup>Corresponding author.

Contributed by the Manufacturing Engineering Division of ASME for publication in the JOURNAL OF MICRO- AND NANO-MANUFACTURING. Manuscript received November 3, 2018; final manuscript received March 19, 2019; published online July 25, 2019. Assoc. Editor: Irene Fassi.

In this study, ultrasonic vibration-assisted burnishing (UVAB) was used to process AM metal parts. Ball burnishing has been used as a finishing process because it can enhance the surface quality [7]. The surface layer of workpiece material is plastically deformed by the force from the burnishing tool [8]. It is reported that burnishing can improve not only surface roughness [9–11] but also wear resistance [9] and corrosion resistance. Furthermore, a burnished surface has compressive residual stress [9,12], which contributes to the improvement of fatigue strength [7]. Because of these unique effects, burnishing has been applied to some special applications such as injection molds fabrication [13]. Also, applying ultrasonic vibration (UV) to a burnishing tool is known to effectively enhance the burnishing effect by improving surface roughness, hardness, and residual stress [14]. With UV assistance, burnishing can be performed at a lower force as compared with conventional burnishing [8]. The UVAB for AM samples has also been attempted in recent years [3,4,15–17]. However, up to date, how the UV assistance affects the material deformation behavior beneath the burnishing tool has not been clarified. Moreover, in a ball burnishing process, the shape of a ball tool is transferred to the workpiece, causing the formation of arcs and cusps on the workpiece surface and an increase in surface roughness [7]. To solve this problem, it is important to optimize the lateral pass width of the tool, namely the distance between two successive adjacent burnishing passes.

In this study, UVAB was performed on AM AlSi10Mg samples, and the effect of vibration amplitude and lateral pass width on the resulting surface topography and hardness, as well as burnishing forces, was investigated. Cross-sectional morphology of the burnished sample was observed by X-ray micro-CT and the change in filling ratio was obtained. The findings from this study will demonstrate the possibility of improving the surface and subsurface integrity of metal parts produced by AM in a single-step process.

## 2 Experiment

Figure 1 shows a schematic diagram of material structural change in UVAB. It is expected that UVAB can reduce internal voids and surface roughness simultaneously, as well as induce compressive residual stress in the surface layer. To realize this objective, a UVAB system was built in this study, the schematic and photograph of which are shown in Fig. 2. An ultrasonic vibration spindle made by SEEG Co., Ltd., Japan, was attached to a four-axis simultaneous control stage L4S-300 made by Sodick Co., Ltd., Japan. The structure of UV spindle unit is shown in Fig. 3, where a piezoelectric element is used as a transducer. To generate ultrasonic vibration, an alternating current was applied from an ultrasonic oscillator to the piezoelectric element. The oscillator used was GSD20AT made by Sonic Technology Co., Ltd., Japan. The amplitude of vibration was measured by a laser displacement gauge, and the result is shown in Fig. 4. The vibration amplitude was about 0.8  $\mu\text{m}$ .

An AM AlSi10Mg block (10 mm  $\times$  10 mm  $\times$  5 mm) was fabricated with a building layer thickness of 30  $\mu\text{m}$  using the EOSINT M280 3D printing machine made by EOS GmbH, Germany. The

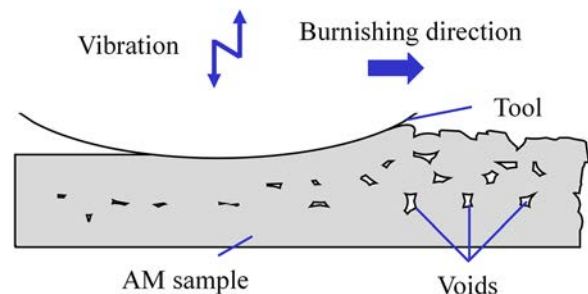
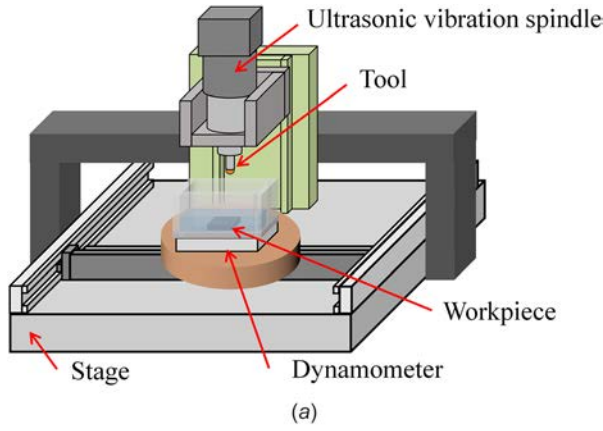
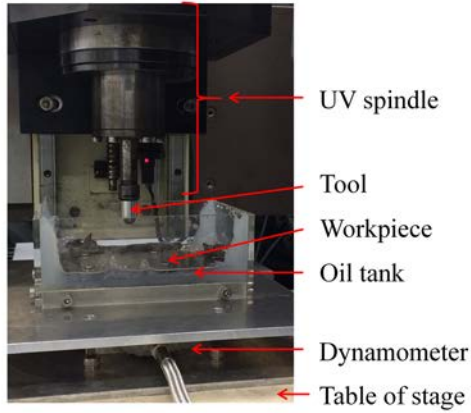


Fig. 1 Schematic diagram of UVAB for AM metals



(a)



(b)

Fig. 2 (a) A schematic diagram and (b) a photograph of the experimental setup

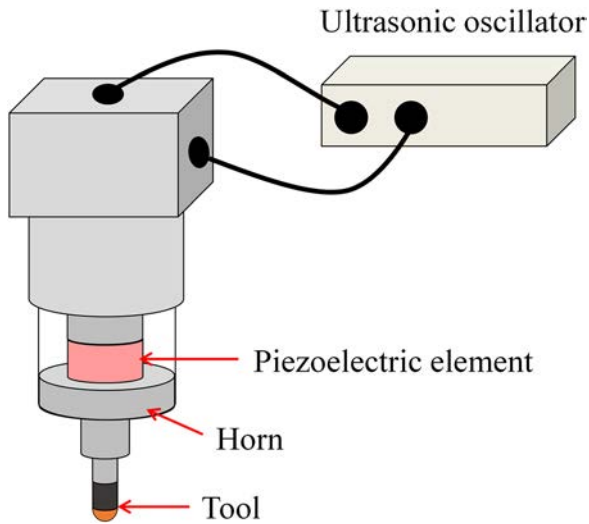


Fig. 3 Structure of the ultrasonic vibration unit

block was then divided into four equal parts (5 mm × 5 mm × 5 mm) for the burnishing experiments. The burnishing tool used in this study was self-made in the laboratory, as shown in Fig. 5. A polished ceramic ball of silicon nitride made by Tsubaki Nakashima Co., Ltd., Japan, was fixed to an end of a steel shaft. The ball diameter is 10 mm, surface roughness <math>< 50 \text{ nmRa}</math>, and Vickers hardness 1600 HV. In burnishing process, the shape of the tool is transferred to the sample, so the surface condition of the tool is crucial. Since the ball is much smoother and harder than the AM metal sample, the

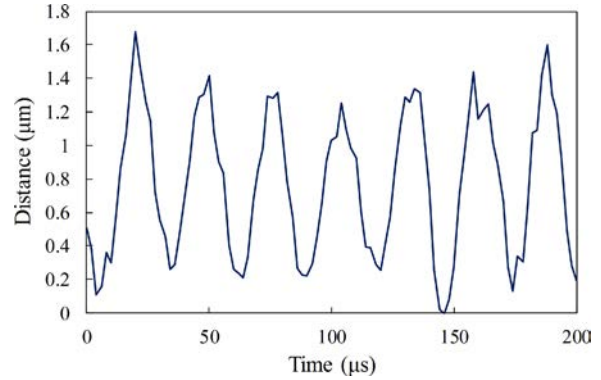


Fig. 4 Measured amplitude of ultrasonic vibration

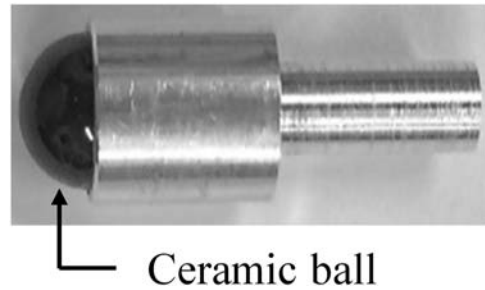


Fig. 5 Photograph of the burnishing tool used in experiment

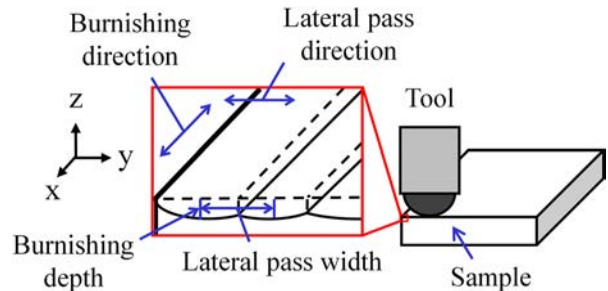


Fig. 6 Schematic model of surface generation in burnishing

surface condition of the tool will be maintained throughout the experiment.

A model of surface generation in UVAB is illustrated in Fig. 6, where the definitions of important parameters, such as burnishing direction and lateral pass width, are indicated. In this study, the burnishing direction was set parallel to the laser scanning direction on the top surface, while the lateral pass direction perpendicular to the laser scanning direction.

Table 1 shows the conditions used in the experiments. The effect of UV assistance was investigated by comparing the results without and with UV (experiments A and B). In addition, the effect of lateral pass width in UVAB was also investigated (experiment C). The burnishing depth and lateral pass width were fixed at 0.5 mm during the process in experiments A and B, while they were changed in experiment C. In Table 1, depth and time of burnishing are shown as  $a \mu\text{m} \times b$  times. This means burnishing is performed for  $b$  times and the burnishing depth was increased by  $a \mu\text{m}$  for each time. In experiment C, burnishing was performed under condition (1) followed by condition (2). In order to improve the lubricity between the tool and the sample, machining oil Shell Paraol 250 made by SHOWA SHELL SEKIYU K. K., Japan, was used.

To judge the surface quality improvement, surface morphology, surface roughness, cross-sectional morphology, and filling ratio

**Table 1 Experimental conditions**

Experiment No.	A	B	C
Ultrasonic vibration	No	Yes	Yes
Workpiece material	AM AlSi10 Mg		
Tool feed rate	10 mm/s		
Lubricant	Machining oil		
Vibration frequency	27 kHz		
Vibration amplitude	0.8 $\mu\text{m}$		
Depth and time of burnishing	30 $\mu\text{m}$ $\times$ 14 times	(1) 30 $\mu\text{m}$ $\times$ 13 times (2) 1 $\mu\text{m}$ $\times$ 10 times	
Lateral pass width	0.5 mm	(1) 0.5 mm (2) 0.1 mm	

were evaluated. Surface morphology of samples was observed by a scanning electron microscope (SEM) Inspect S50 made by FEI Company (Hillsboro, OR). Surface roughness was measured by a laser probe unit MP-3 made by Mitaka Kohki Co., Ltd. (Tokyo, Japan). Sampling length was 9 mm for untreated surface and 4 mm for treated surfaces, and measurement was carried out for five times for each sample. Cross-sectional morphology was observed by X-ray micro-CT SKYSCAN 1272 made by Bruker Corporation (Billerica, MA). Filling ratio was then obtained from the X-ray scan images, using CT-Analyzer software. Furthermore, the change in Vickers hardness was measured using a micro-Vickers hardness tester HMV-G21 made by Shimadzu Corporation (Kyoto, Japan). There is a correlation between fatigue strength and hardness [18]. The Vickers hardness test was performed five times consecutively for each sample at a static load of 490 mN with a hold for 10 s. During burnishing, a compact multi-component piezoelectric dynamometer 9256C2 made by Kistler Co, Ltd. (Winterthur, Switzerland) was used to measure the burnishing forces in experiment A and B to investigate the effect of UV assistance. Sampling period was set to 200  $\mu\text{s}$ .

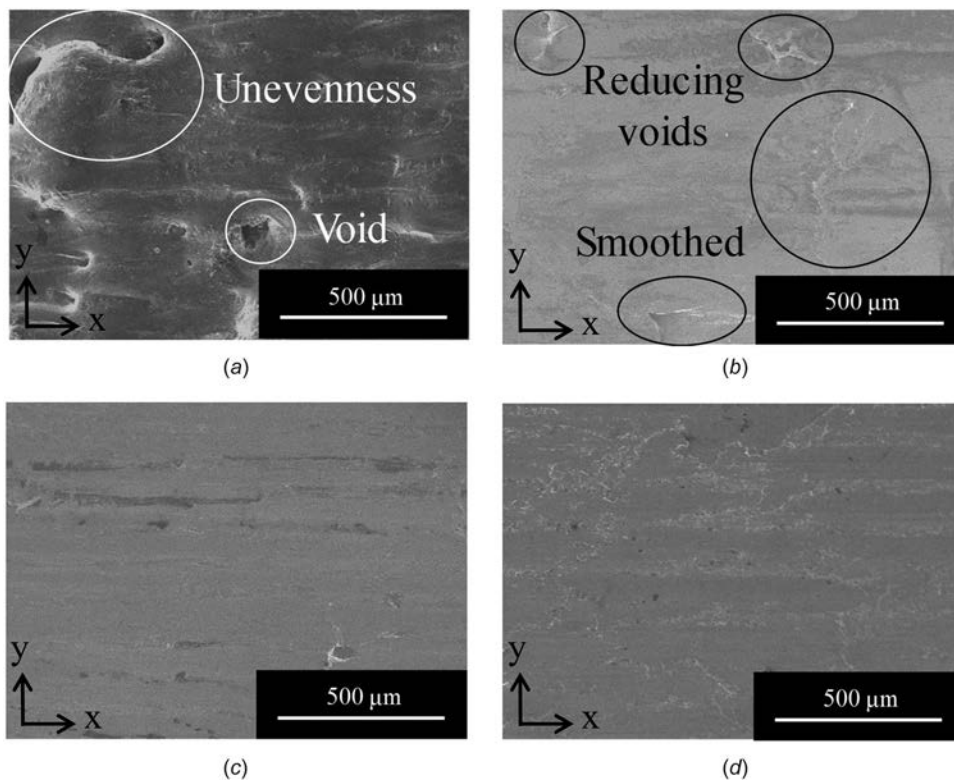


**Fig. 7 SEM images of untreated and treated surfaces by burnishing: (a) untreated, (b) experiment A, (c) experiment B, and (d) experiment C (x—burnishing direction, y—lateral pass direction)**

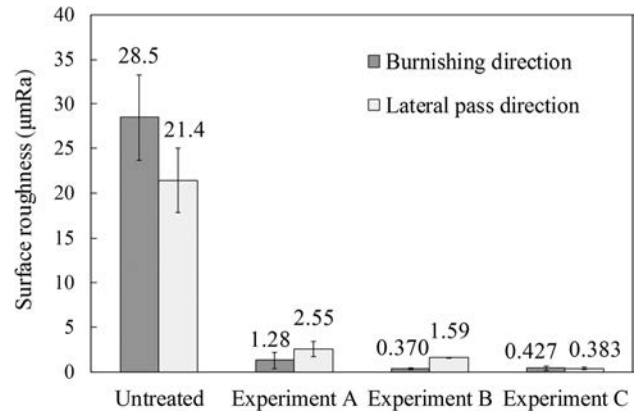


**Fig. 8 Change of surface roughness under various burnishing conditions**

### 3 Results and Discussion

**3.1 Surface Morphology.** The SEM photographs for untreated and treated surfaces are shown in Fig. 7. In Fig. 7(a), it is observed that the surface without treatment has uneven areas and several voids, which makes the surface very rough. However, as shown in Figs. 7(b)–7(d), the surfaces have been greatly smoothed out after burnishing. At the same time, the voids are also filled, as they became smaller or were eliminated. There is not much difference among Figs. 7(b)–7(d). From these results, it can be concluded that the surface morphology was greatly improved by the burnishing process.

**3.2 Surface Roughness.** The results of surface roughness measurements are summarized in Fig. 8. Compared with the sample before treatment, the roughness was greatly improved by the burnishing process. This improvement occurred even without UV

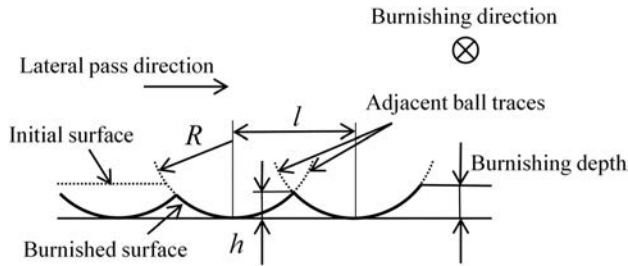


Fig. 9 Surface cusp formation in ball burnishing

assistance (experiment A). However, UV assistance enhanced the improvement of the surface roughness as demonstrated in experiments B and C compared with experiment A. This result indicates that UV assistance is significant in improving surface roughness, which is consistent with previous studies [4,19].

Concerning experiment B, there is variation in surface roughness depending on measurement direction, whereas experiment C shows no variation. As mentioned in Sec. 2, since the shape of the tool is transferred to the workpiece during burnishing, it results in the formation of arcs on the surface in a lateral pass direction as shown in Fig. 9. Furthermore,  $h$  in Fig. 9 is calculated by Eq. (1) [20], which is often used in predicting surface roughness [10]

$$h = \frac{125 l^2}{R} \quad (1)$$

In Eq. (1),  $h$  is the maximum height of a cusp in micrometer;  $l$  is lateral pass width in mm; and  $R$  is the radius of the burnishing ball in mm. Using Eq. (1),  $h$  in experiments B and C (1) was calculated to be  $6.25 \mu\text{m}$ , while  $0.25 \mu\text{m}$  in experiment C (2). By changing a lateral pass width from 0.5 mm to 0.1 mm, theoretical  $h$  varies by a factor of 25. The surface profiles for experiments B and C are shown in Fig. 10. In Fig. 10(a), the transfer of the ball shape is obvious. A periodical pattern is formed every 0.5 mm with  $h$  of  $5.5\text{--}6.0 \mu\text{m}$ , which almost coincides with the applied lateral pass width (0.5 mm) and the calculated value  $h$  ( $6.25 \mu\text{m}$ ). These facts indicate that the higher surface roughness is due to transfer of the tool shape. On the other hand, there is no periodical pattern in Fig. 10(b). The measured value  $h$  was about  $1\text{--}2 \mu\text{m}$ . Though the measured value is bigger than the calculated value ( $0.25 \mu\text{m}$ ), the result suggests that the effect of tool shape transfer on surface roughness has been greatly reduced by applying a smaller lateral pass width. It should be noted that a smaller lateral pass width leads to a longer processing time and should not be used from the first step. In burnishing for AM metals, applying a smaller lateral pass width in only latter steps is preferable such as in experiment C, where the surface roughness was improved by 98% on both directions.

**3.3 Cross-Sectional Morphology.** The observed cross section by X-ray micro-CT is shown in Fig. 11. The upper part of each cross section is the treated part. Before treatment (Fig. 11(a)), an uneven surface was observed, but the surface was smoothed out after burnishing (Figs. 11(b)–11(d)). This fact supports the conclusion that the burnishing process is effective for improving surface roughness as discussed in Secs. 3.1 and 3.2. After burnishing, the top surface became slight bow shaped. This is due to the side flow of material at the workpiece edges.

Before treatment, voids were observed in subsurface region (Fig. 11(a)). After treatment, however, the voids in were reduced or completely eliminated by burnishing. In Figs. 11(b)–11(d), voids larger than  $100 \mu\text{m}$  were eliminated within a depth range of  $500 \mu\text{m}$  from the surface. In experiment A, some smaller voids in  $10 \mu\text{m}$  level size still exist as indicated by the red circles in Fig. 11(b), but such voids were eliminated under experiments B and C. The elimination of voids by UV assistance is significant to

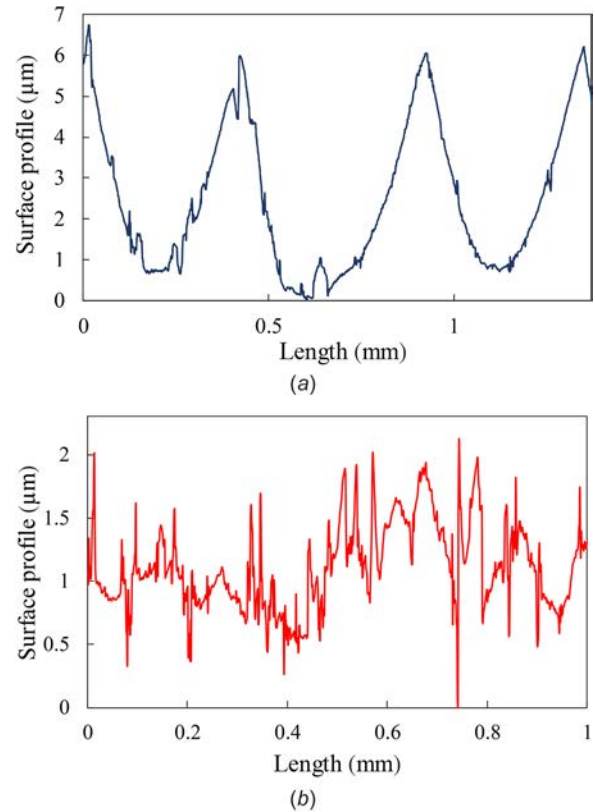


Fig. 10 Surface roughness profiles along lateral pass direction in UVAB: (a) experiment B and (b) experiment C

suppress crack initiation and propagation, which contributes to enhancing fatigue strength [3].

**3.4 Filling Ratio.** Filling ratio was calculated using Eq. (2) at a step of every  $200 \mu\text{m}$  depth from the workpiece surface on the cross section observed by X-ray micro CT

$$\text{Filling ratio} = \frac{S_t}{S_t + S_v} \quad (2)$$

In Eq. (2),  $S_v$  is the area of voids and  $S_t$  is the total area of a sample cross section. The measurement results of the filling ratio are shown in Fig. 12. Without any treatments, the filling ratio was about 90%. After burnishing, the filling ratio becomes obviously higher near the surface. This shows that the effect of material densification becomes stronger at a location closer to the surface. This trend agrees with the depth-gradient nature of hardness [3], indicating that a gradient distribution of plastic strain was induced by burnishing.

Additionally, a comparison among experiments A–C in Fig. 12 shows that greater densities were obtained after treatment using UV assistance. Without UV assistance, the filling ratio shows almost no change when the depth from surface is larger than 0.8 mm (experiment A). When UV assistance is applied, however, the filling ratio keeps decreasing even the depth from surface is larger than 1.2 mm (experiments B and C). This implies that voids have been filled out at a deeper region by burnishing with UV assistance than that without UV assistance. This might have been caused by the UV-induced promotion of dislocation movement [21]. In UVAB, the surface is hammered vertically with strong impacts repeatedly. By this so-called hammering effect, the inside of the samples was deformed significantly [22]. It should be noted that although the burnishing depth in experiment C was smaller, it induced a higher material density than experiment B. This may

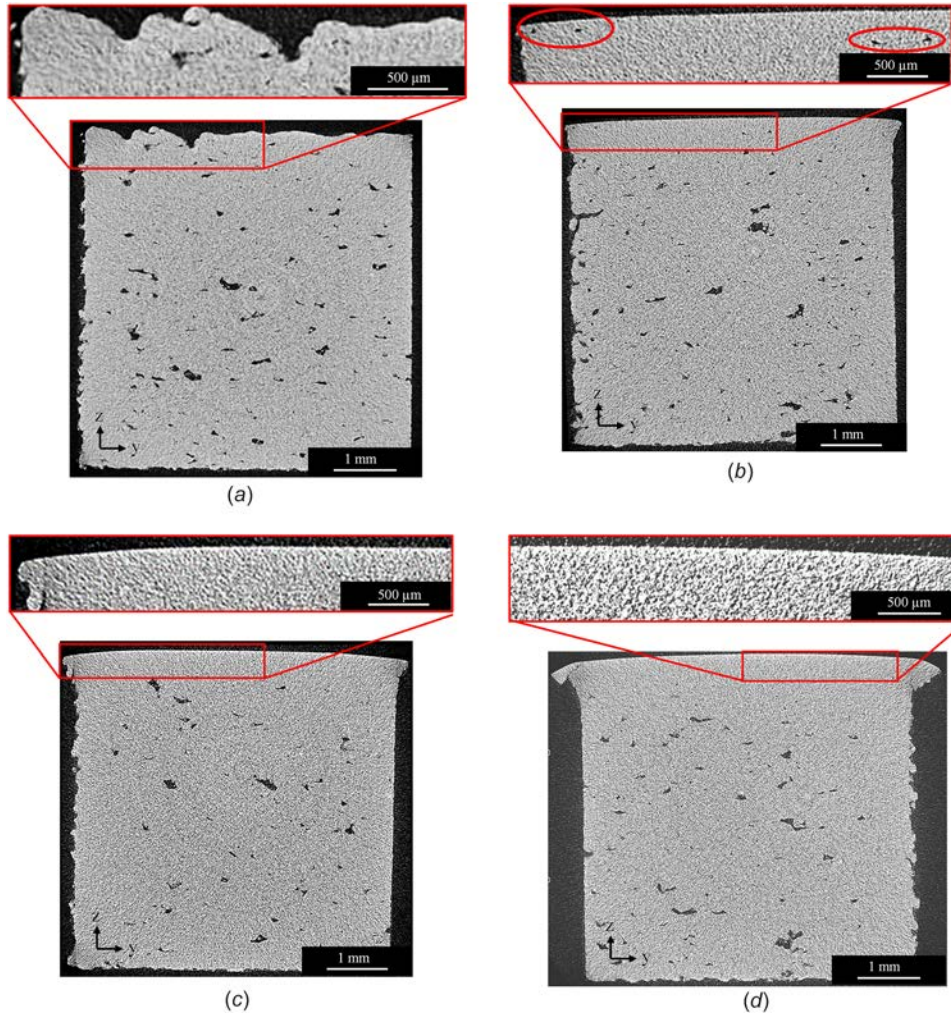


Fig. 11 Cross-sectional images of the samples before/after burnishing: (a) untreated, (b) experiment A, (c) experiment B, and (d) experiment C

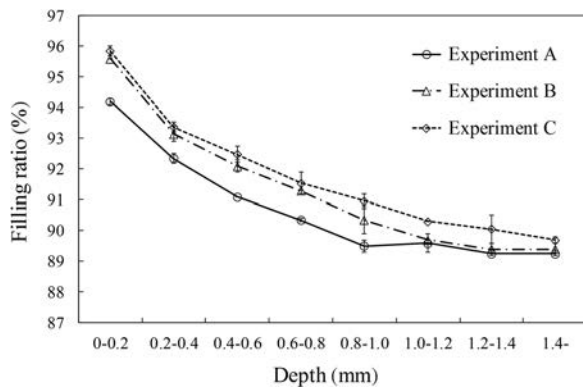


Fig. 12 Change of filling ratio with burnishing depth under various conditions

have been caused by the smaller lateral pass width used in experiment C.

**3.5 Vickers Hardness.** The hardness results are shown in Fig. 13. Experiment A resulted in a 2.4% improvement of hardness compared to the untreated surface. This small increase in hardness should be due to work hardening [23]. On the other hand, greater improvement of hardness by 13% and 24% were

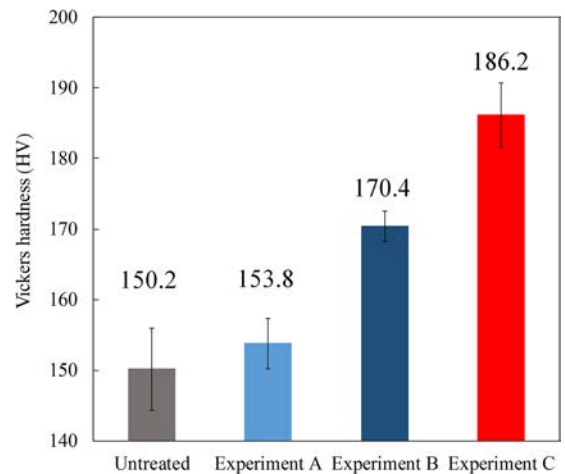
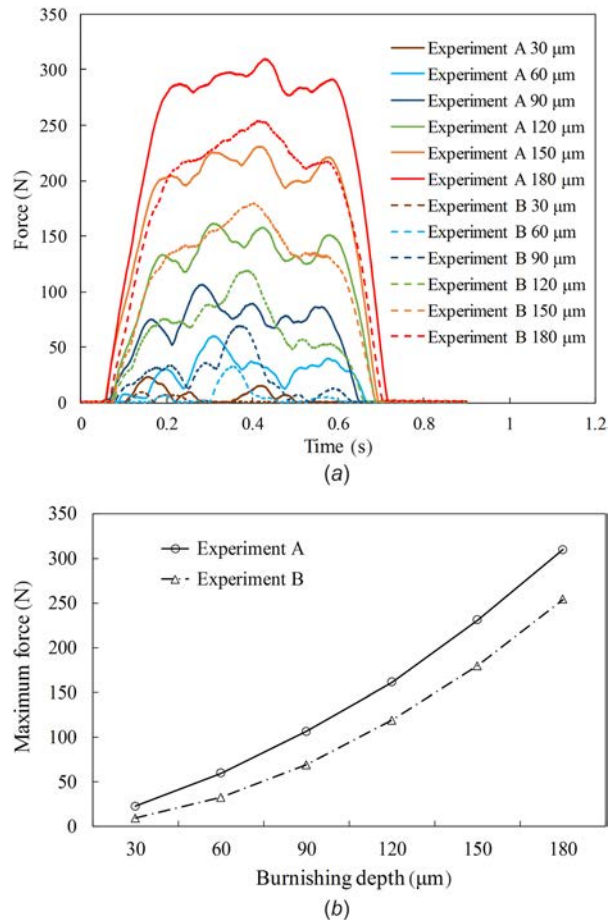


Fig. 13 Change in Vickers hardness with burnishing conditions

obtained in experiments B and C, respectively, when UV assistance was applied. This indicates that UV assistance is very helpful in improving surface hardness. This effect was caused by repetitive deformation by UV [24]. The dislocation density increases during UVAB, so the plastic deformation during the



**Fig. 14 Burnishing force results in experiments A and B: (a) raw data for each experiment and (b) maximum forces measured in all experiments**

Vickers hardness tests is hindered and a higher hardness value is measured. In addition, the UVAB-induced grain refinement [21,25] and void reduction [3] may also cause hardness increase.

**3.6 Burnishing Force.** The burnishing force measurement results are shown in Fig. 14. Figure 14(a) shows raw data for each condition, and Fig. 14(b) summarizes the maximum forces measured in all conditions. The force was measured at a step of  $30\ \mu\text{m}$  of burnishing depth under experiments A and B. The result shows that the maximum force increases with the burnishing depth. In comparison between experiments A and B, experiment B shows a lower force. This is due to the effect of UV, as reported in previous studies [26]. That is to say, the intermittent contact caused by UV reduces the average force.

**3.7 Tool Wear.** Finally, to examine possible tool wear, the cross-sectional profile passing through the tip of the tool was measured after burnishing experiments, as shown in Fig. 15(a). Figure 15(b) shows the distribution of form error between the ideal profile with a diameter of 10 mm and the measured profile in Fig. 15(a). In Fig. 15(a), the tip of the tool is at a height of 0.1 mm, and the tool–workpiece contact area is from 0.1 mm to 0.07 mm ( $30\ \mu\text{m}$  from the tool tip). The shape change of the contact area compared to the noncontact area is extremely small. In Fig. 15(b), the form error profile is flat with submicron level variations between the contact area (a distance of 0.5–1.5 mm) and the noncontact area (a distance of 0–0.5 mm and 1.5–2 mm), showing the tool wear was insignificant in the UVAB process.

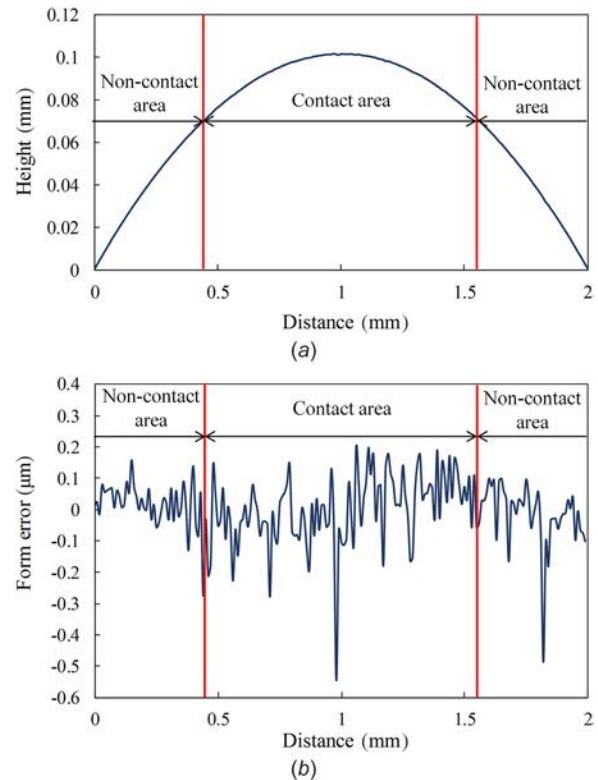


**Fig. 15 Surface profiles of the burnishing tool after experiments: (a) cross-sectional profile raw data and (b) distribution of form error between the ideal profile and the measured profile**

## 4 Conclusions

Ultrasonic vibration-assisted burnishing was conducted for additive-manufactured AlSi10Mg samples to improve the surface and subsurface integrity. Tool shape affects surface roughness, but it was possible to reduce the tool shape effect by using a sufficiently small lateral pass width. Surface roughness was improved by 98% for both burnishing direction and lateral pass direction. It was also possible to eliminate a greater number of voids at a greater depth using ultrasonic vibration assistance. Furthermore, the ultrasonic vibration assistance also improved the hardness of samples by 24% and reduced the burnishing force. The results from this study demonstrate the possibility of significant improvement of the surface quality of additive manufactured metal products by ultrasonic vibration-assisted burnishing.

## References

- [1] Frazier, W. E., 2014, "Metal Additive Manufacturing: A Review," *J. Mater. Eng. Perform.*, **23**(6), pp. 1917–1928.
- [2] Rannar, L. E., Glad, A., and Gustafson, C. G., 2007, "Efficient Cooling With Tool Inserts Manufactured by Electron Beam Melting," *Rapid Prototyp. J.*, **13**(3), pp. 128–135.
- [3] Ma, C., Andani, M. T., Qin, H., Moghaddam, N. S., Ibrahim, H., Jahadkbar, A., Amerintanazi, A., Ren, Z., Zhang, H., Doll, G. L., Dong, Y., Elahinia, M., and Ye, C., 2017, "Improving Surface Finish and Wear Resistance of Additive Manufactured Nickel-Titanium by Ultrasonic Nano-Crystal Surface Modification," *J. Mater. Process. Technol.*, **249**, pp. 433–440.
- [4] Zhang, H., Chiang, R., Qin, H., Ren, Z., Hou, X., Lin, D., Doll, G. L., Vasudevan, V. K., Dong, Y., and Ye, C., 2017, "The Effects of Ultrasonic Nanocrystal Surface Modification on the Fatigue Performance of 3D-Printed Ti64," *Int. J. Fatigue*, **103**, pp. 136–146.
- [5] Guo, N., and Leu, M. C., 2013, "Additive Manufacturing: Technology, Applications and Research Needs," *Front. Mech. Eng.*, **8**(3), pp. 215–243.
- [6] Yasa, E., Deckers, J., Kruth, J. P., Yasa, E., Deckers, J., and Kruth, J., 2011, "The Investigation of the Influence of Laser Re-Melting on Density, Surface Quality and Microstructure of Selective Laser Melting Parts," *Rapid Prototyp. J.*, **17**(5), pp. 312–327.

- [7] Gomez-Gras, G., Travieso-Rodríguez, J. A., Jerez-Mesa, R., Lluma-Fuentes, J., and Gomis de la Calle, B., 2016, "Experimental Study of Lateral Pass Width in Conventional and Vibrations-Assisted Ball Burnishing," *Int. J. Adv. Manuf. Technol.*, **87**, pp. 363–371.
- [8] Travieso-Rodríguez, J. A., Gomez-Gras, G., Dessein, G., Carrillo, F., Alexis, J., Jorba-Peiro, J., and Aubazac, N., 2015, "Effects of a Ball-Burnishing Process Assisted by Vibrations in G10380 Steel Specimens," *Int. J. Adv. Manuf. Technol.*, **81**(9–12), pp. 1757–1765.
- [9] Revankar, G. D., Shetty, R., Rao, S. S., and Gaitonde, V. N., 2017, "Wear Resistance Enhancement of Titanium Alloy (Ti-6Al-4V) by Ball Burnishing Process," *J. Mater. Res. Technol.*, **6**(1), pp. 13–32.
- [10] Bouzid, W., Tsoumarev, O., and Saï, K., 2004, "An Investigation of Surface Roughness of Burnished AISI 1042 Steel," *Int. J. Adv. Manuf. Technol.*, **24**(1), pp. 120–125.
- [11] Shiou, F. J., and Banh, Q. N., 2016, "Development of an Innovative Small Ball-Burnishing Tool Embedded With a Load Cell," *Int. J. Adv. Manuf. Technol.*, **87**(1–4), pp. 31–41.
- [12] John, M. R. S., Wilson, A. W., Bhardwaj, A. P., Abraham, A., and Vinayagam, B. K., 2016, "An Investigation of Ball Burnishing Process on CNC Lathe Using Finite Element Analysis," *Simul. Model. Pract. Theory*, **62**, pp. 88–101.
- [13] Shiou, F. J., and Chen, C. H., 2003, "Freeform Surface Finish of Plastic Injection Mold by Using Ball-Burnishing Process," *J. Mater. Process. Technol.*, **140**(1–3), pp. 248–254.
- [14] Huuki, J., and Laakso, S. V. A., 2013, "Integrity of Surfaces Finished With Ultrasonic Burnishing," *Proc. Inst. Mech. Eng. Part B*, **227**(1), pp. 45–53.
- [15] Salmi, M., Huuki, J., and Ituarte, I. F., 2017, "The Ultrasonic Burnishing of Cobalt-Chrome and Stainless Steel Surface Made by Additive Manufacturing," *Prog. Addit. Manuf.*, **2**(1–2), pp. 31–41.
- [16] Kattoura, M., Telang, A., Mannava, S. R., Qian, D., and Vasudevan, V. K., 2018, "Effect of Ultrasonic Nanocrystal Surface Modification on Residual Stress, Microstructure, and Fatigue Behavior of ATI 718Plus Alloy," *Mater. Sci. Eng. A*, **711**, pp. 364–377.
- [17] Ye, C., Telang, A., Gill, A., Wen, X., Mannava, S. R., Qian, D., and Vasudevan, V. K., 2018, "Effects of Ultrasonic Nanocrystal Surface Modification on the Residual Stress, Microstructure, and Corrosion Resistance of 304 Stainless Steel Welds," *Metall. Mater. Trans. A*, **49**(3), pp. 972–978.
- [18] Casagrande, A., Cammarota, G. P., and Micele, L., 2011, "Relationship Between Fatigue Limit and Vickers Hardness in Steels," *Mater. Sci. Eng. A*, **528**(9), pp. 3468–3473.
- [19] Gomez-Gras, G., Travieso-Rodríguez, J. A., Gonzalez-Rojas, H. A., Napoles-Alberro, A., Carrillo, F. J., and Dessein, G., 2015, "Study of a Ball-Burnishing Vibration-Assisted Process," *Proc. Inst. Mech. Eng. Part B*, **229**(1), pp. 172–177.
- [20] Bouzid Saï, W., and Saï, K., 2005, "Finite Element Modeling of Burnishing of AISI 1042 Steel," *Int. J. Adv. Manuf. Technol.*, **25**(5–6), pp. 460–465.
- [21] Liu, J., Suslov, S., Li, S., Qin, H., Ren, Z., Ma, C., Wang, G.-X., Doll, G. L., Cong, H., Dong, Y., and Ye, C., 2017, "Effects of Ultrasonic Nanocrystal Surface Modification on the Thermal Oxidation Behavior of Ti6Al4V," *Surf. Coat. Technol.*, **325**, pp. 289–298.
- [22] Mordyuk, B. N., and Prokopenko, G. I., 2007, "Ultrasonic Impact Peening for the Surface Properties' Management," *J. Sound Vib.*, **308**(3–5), pp. 855–866.
- [23] Hassan, A. M., and Al-Bsharat, A. S., 1996, "Influence of Burnishing Process on Surface Roughness, Hardness, and Microstructure of Some Non-Ferrous Metals," *Wear*, **199**(1), pp. 1–8.
- [24] Bozdana, A. T., Gindy, N. N. Z., and Li, H., 2005, "Deep Cold Rolling With Ultrasonic Vibrations—A New Mechanical Surface Enhancement Technique," *Int. J. Mach. Tools Manuf.*, **45**(6), pp. 713–718.
- [25] Zhao, J., and Liu, Z., 2016, "Investigations of Ultrasonic Frequency Effects on Surface Deformation in Rotary Ultrasonic Roller Burnishing Ti-6Al-4V," *Mater. Des.*, **107**, pp. 238–249.
- [26] Akbari, J., Borzoei, H., and Mamduhi, M. H., 2008, "Study on Ultrasonic Vibration Effects on Grinding Process of Alumina Ceramic (Al<sub>2</sub>O<sub>3</sub>)," *Int. J. Mech. Aerosp. Ind. Mechatronic Manuf. Eng.*, **2**(5), pp. 722–726.